DOI: 10.71762/symb-ra67

Research Paper

Investigation of the Stamping Process of The Jack Bracket of The Kia Rio Car

Peyman Mashhadi Keshtiban[1*], Ali Fata[2]

[1]Faculty of Mechanical Engineering, Urmia University of Technology, Urmia, Iran

[2]Department of Mechanical Engineering, Faculty of Engineering, University of Hormozgan, Bandar Abbas, Iran

[*]Email of the Corresponding Authors: m.keshtiban@mee.uut.ac.ir

Received: October 13, 2024; Accepted: December 16, 2024

Abstract

Sheet metal forming is one of the main processes of forming thin-walled plates to produce the semi-final and final parts with high precision. In the present work, a complete investigation of the forming operation of the jack bracket of the Kia Rio car has been conducted with the help of the Design of Experiment (DOE) method, numerical simulations, and experimental investigations. First, the Finite Element (FE) method performed a numerical simulation of the process, and the results were compared with experimental results. Then, 13 proposed simulations were performed through the Box-Behnken experimental design method to study the effect of process parameters. The Friction Coefficient (FC), the press speed, and the Blank Holder Force (BHF) were chosen as input parameters. The maximum strain, the maximum stress of the part and the maximum punch force were considered output parameters. The results indicated that punch speed had the most significant effect on the plastic strain, with a contribution of 61.63%, and also FC had the most impact on the maximum force, with a contribution of 58.69%. Moreover, the role of BHF in the mentioned outputs was not considerable, but it was significant (31.47%) in the investigation of stresses.

Keywords

Stamping, FEM, DOE, Box-Behnken

Abbreviations

DOE	Design of Experiment
FC	Friction Coefficient
BHF	Blank Holder Force
PEEQ	Equivalent Plastic Strain
FE	Finite Element
R^2	the coefficient of determination, R squared
R^2_{Adj}	Adjusted R^2
R^2_{Pre}	Predicted R^2
df	Degrees of freedom

1. Introduction

Nowadays, producing parts with complex shapes and low cost, considering high environmental considerations, are among the main challenges of the manufacturing industries, especially the automotive industry. The realization of this objective requires the development of technology, especially in the metal-forming industry. Metal sheets, with many advantages, such as high modulus of elasticity and yield strength, produce parts with a high strength-to-weight ratio. It is noteworthy that in today's modern and industrial world, stamping, or forming metal sheets, has been extensively developed to meet the above requirements. Moreover, newly developed technologies in controlling the thickness and dimensional accuracy of the product have many industrial applications. Since metal forming processes contain various input and output parameters, FE is a powerful tool to predict and optimize metal forming processes [1-6]. In the automotive research center, the hot stamping process was simulated by FE analysis to make weight-saving improvements and enhance crash performance [7]. Firat [8] modeled the sheet stamping process by the Ls-Dyna FE code. It was concluded that selecting the element type depends on the computer resources and FE code capabilities. High-strength steel was defamed by a hot stamping process and simulated by FE by Zhang et al. [9]. Hot deformation processes are simulated when the behavior of the metal is defined by various high-temperature experimental works [10]. In another study, Kim [11] simulated fatigue characteristics and lightweight design of automotive knuckles by FE. 6061-T6 aluminum alloy as a lightweight material was suggested as the substitution for FCD600 cast iron material, and careful studies were conducted to determine whether to use it. Zhou et al. [12] studied another numerical simulation on tailored hot stamping of boron steel by partial heating. Zerilli Armstrong's constitutive equations defined hot deformation behavior. Integrated with finite element simulations, various frictional behavior models of pure titanium thin sheet in stamping process was investigated be wang et al. [13]. It was concluded that the proposed friction model improves efficiency and accuracy. Modanloo et al. [14] studied the formability of stamped titanium bipolar plates. Critical process parameters, namely die clearance, forming speed, and sheet/die friction coefficient, are considered input parameters. For this purpose, experiments on the FE model and the response surface method (RSM) were applied. Also, the stamping of automotive parts was successfully studied and recommended by FE simulation together with experimental results in other works [15-16]. The previous works investigation outcome revealed that various and not categorized methods and tools in the stamping process of car parts used before. Then, in the present work, a complete and detailed investigation of stamping operation of the jack bracket part of the Kia Rio car has been carried out with numerical simulation, experimental test, and DOE method. First, the numerical simulation of the process was performed using the FE method in ABAQUS, and the results were compared to the experimental results. Then, thirteen proposed simulations have been performed using the Box-Behnken method to study the effectiveness of process parameters. The input parameters such as FC, press speed, and BHF, and output parameters such as maximum part strain, maximum part stress, and maximum punch force, have been taken into account. In order to achieve the proposed goal, in the next step materials and methods that have been used explain in detail. Then, results of introduced methods will be compared and discussed in detail.

2. Materials and Methods

2.1. Experimental Tests

The initial plate of a 2.0 mm thick steel sheet made of ST-37 is cut by a guillotine machine in 400×400 mm^2 dimensions. In the next step of the stamping process, the sheet is placed under the pressure of a 100-ton hydraulic press between the two halves of the preformed mold, creating the initial form on the sheet, Figure. 1. Finally, the main part is obtained after performing the final forming step and cutting the extra edges (Figure 1c).

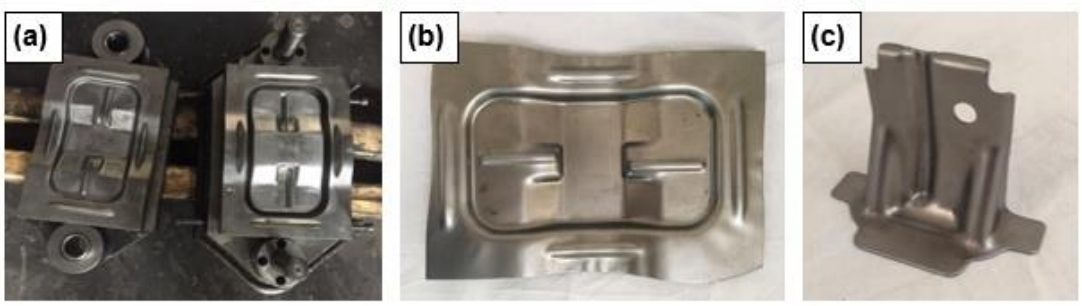

Figure 1. a) Die halves in the first step of jack bracket, b) Semi-final workpiece after the first step of the process, and c) final part of jack bracket

2.2 FE Simulation

Finite element analysis is usually used in different studies to predict the objective functions and reduce experimental costs [17-19]. Then, the preformed stamping process has been simulated by FE in three-dimensional form using the cold-worked plane strain method. Essential and practical parameters of this process, such as press speed, FC, and BHF, have been analyzed and reviewed during various experiments. The dies for producing this part were made of tool steel H13, and the physical and mechanical properties of the dies are listed in Table 2.

Table 2. Physical and mechanical properties of tool steel H13 [20]

Properties	Metric
Tensile Strength, Ultimate (@20°C/68°F, Varies With Heat Treatment)	1200-1590 MPa
Tensile Strength, Yield (@20°C/68°F, Varies With Heat Treatment)	1000-1380 MPa
Reduction Of Area (@20°C/68°F)	50.00%
Modulus Of Elasticity (@20°C/68°F)	215 GPa
Poisson's Ratio	0.27-0.3
Density (@20°C/68°F)	7800 Kg/m^3

The properties of the structural equation based on the Johnson-Cook criterion for a 2-mm ST-37 carbon steel sheet are presented in Table 3.

Table 3. Plastic coefficients of Johnson-Cook structural equation used for ST-37 carbon steel [1]

A [MPa]	B [MPa]	m	n	C
255.98	162.58	1	0.2571	0.0220

Mold halves are considered rigid; according to the forming process, all degrees of freedom for the lower mold and deformable sheet were fixed. The upper half moved to shape the part in a straight line, and like the lower half, the other degrees of freedom were fixed. The S4RSW element type has

been used for the workpiece's initial geometry. The name is the abbreviated form of square elements (special for thin shells) with support for plane strain degrees of freedom and small warping consideration by four integration points (to prevent the shear locking phenomenon, common in quasi-static simulations with flexural torque). Due to the use of elements with reduced integration points, the hourglass phenomenon is also possible. In this case, the element cannot sense the bending force due to the inadequate arrangement of integration points, which leads to a significant discrepancy between the analysis results and the unusual deformations of the element. To prevent the hourglass phenomenon, hourglass control was applied to the workpiece elements. As illustrated in Figure. 2, a mesh convergence study was done, and the total number of elements selected was 60214. It is evident that the subjected number of elements should be considered to reach the adequate accuracy of the results, the highest analysis speed, and to satisfy the mesh independency of the finite element model. R3D3 element type has been used in the lower and upper jaws, which are two-dimensional rigid triangular dynamic elements with three integration points in each element.

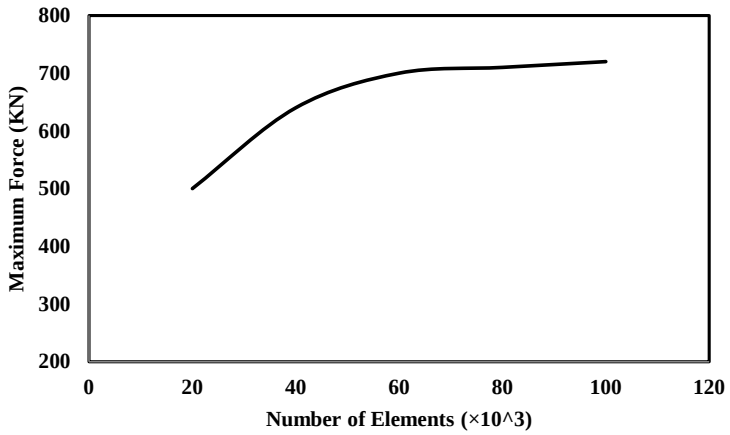

Figure 2. Mesh independency study

2.3 DOE

To estimate the magnitude and nature of the effect of process control parameters, the DOE was applied by response surface method of Box-Behnken arrangement type with quadratic design, 12 midpoints, and one central point (13 experiments in total). According to Table 4, independent input parameters, i.e., punch speed, FC, and BHF, have been known as effective and controllable factors of the process, and the dependent variables, such as Equivalent Plastic Strain (PEEQ), maximum stress, and punch force have also been considered as the corresponding studied Responses.

Table 4. Box-Behnken design

Punch Speed (mm/s)	FC	BHF (KN)
52.5	0.15	500
17.5	0.15	500
35	0.1	500
17.5	0.15	400
52.5	0.2	450
35	0.2	400
17.5	0.2	450
52.5	0.15	400
35	0.1	400
35	0.2	500
17.5	0.1	450
35	0.15	450
52.5	0.1	450

3. Results and discussion

3.1 FE and Experimental Work

In the stamping process, while using brittle sheets with low flexibility, cracks in the bulging back faces are inevitable; however, the desired dimensional accuracy and bending angle can be achieved in several steps using sheets with high ductility. Moreover, based on observations from Figure 3, it is evident that during the operation, the outer edge of the initial sheet tends to be drawn towards the inside, particularly in its middle areas, to provide the mass needed to fill the die. Therefore, it can be concluded that the material tends to be drawn more from the surrounding edges in dies with deeper cavities. In this process, the deformation at the edges is greater than the area in contact with the punch; hence, this area must be lubricated to allow sufficient slipping and prevent rupture. Most of these edges do not contribute to the central part's structure and are cut after the process is completed. However, the optimal selection of tool parameters and initial sheet geometry to fit the part inside the die can yield significant benefits, including increasing the dimensional accuracy of the product and reducing the waste material when designing for mass production. Besides upper comparisons between FE and experimental work, the maximum force needed to produce the part was compared with the simulated outcomes. Results show that there is good conformity between FE and experimental works.

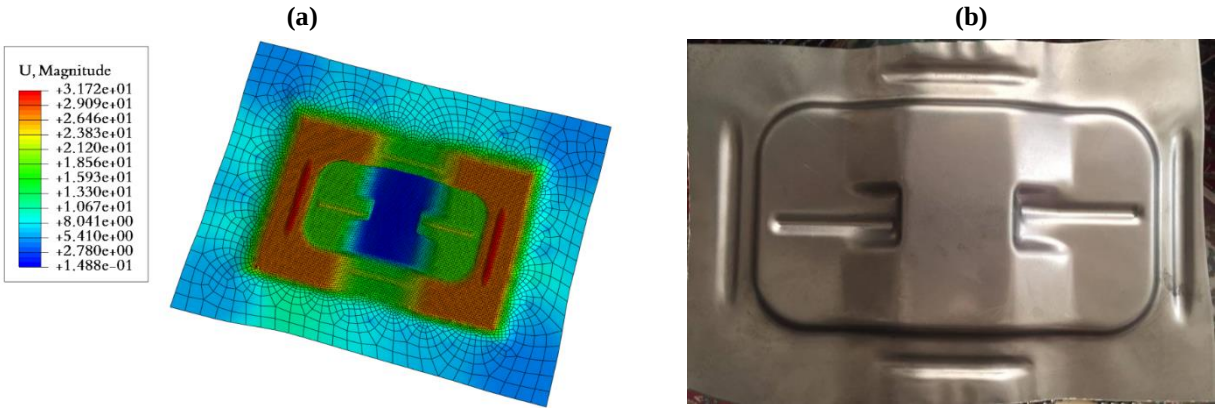

Figure 3. a) Displacement contour (mm) and b) part after stamping

When a punch or jaw containing protrusions applies pressure to the sheet and pushes it into the concavities of the die, it produces tensile forces at the bottom of the notched area. The resultant force causes the deformation and contact stress between the punch and the sheet to be much less than the sheet's yield stress. These tensile forces contribute to increasing the material's strength at the sheet's edge, eventually resulting in annular stresses and shrinking phenomenon. Figure 4. demonstrates the stress contour obtained from the FE analysis of the first stage of the jack bracket's stamping process.

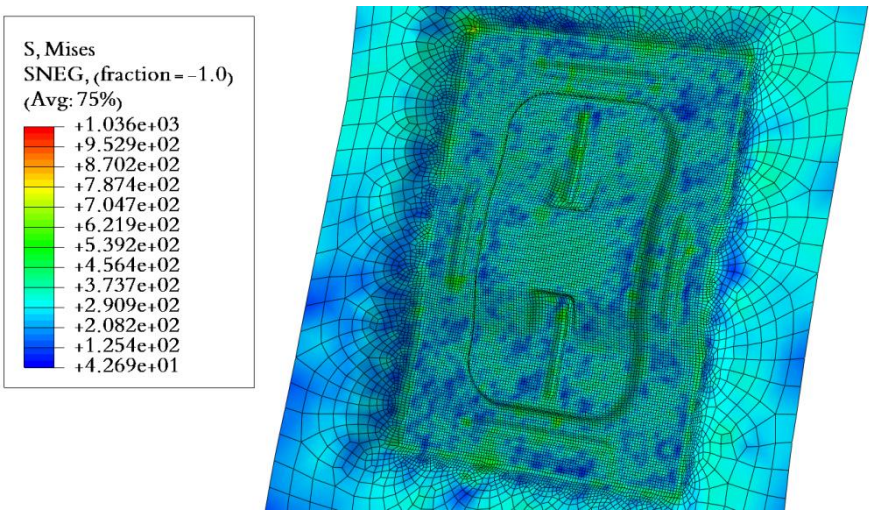

Figure 4. Stress contour after completion of the stamping process of the first stage of the jack bracket (MPa)

Figure 5 indicates the PEEQ contour on the workpiece surface. It is observed that plastic strain occurs in bent areas. No unique plastic deformation occurs in the zones far from bent areas.

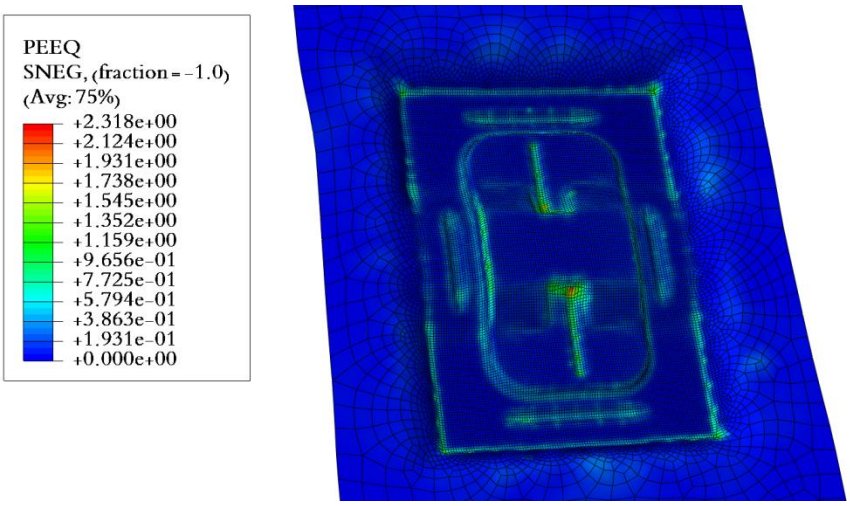

Figure 5. PEEQ contour after completing the stamping process of the first stage of the jack bracket

The force diagram investigation is usually considered in various studies [22]. Then, the force profile during the part formation process is indicated in Figure 6. As can be seen, the pressing force increases logarithmically over time. It reaches its maximum value by completely bending the initial sheet between the protrusions and depressions of the die at the final moments. This maximum value aligns significantly with the data collected from the manufacturer's experimental results. Furthermore, to verify the FE results more, Shang et al. [23] conducted an experimental study of the Electromagnetic pressing process for steel sheets with the exact dimensions and tensile depth and obtained the amount of maximum force, similar to the FE results of this work.

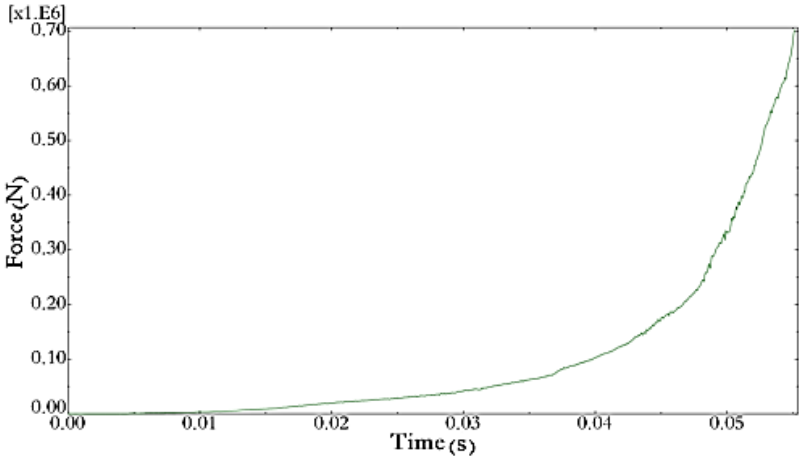

Figure 6. Force profile obtained from FE simulation results

3.2 DOE

The independent input parameters, i.e., punch speed, FC, and BHF, are known as effective and controllable factors of the process, and the dependent variables, PEEQ, maximum stress, and punch reaction force have been considered as the corresponding responses and the results are listed in Table 5.

Table 5. Box-Behnken design and results

Punch Speed (mm/s)	FC	BHF (KN)	Response 1 Max PEEQ	Response 2 Max Stress (MPa)	Response 3 Max Punch Force (KN)
52.5	0.15	500	1.252	617.4	549.1
17.5	0.15	500	1.475	547.2	504.3
35	0.1	500	1.302	539.8	487.9
17.5	0.15	400	1.402	964.0	492.4
52.5	0.2	450	1.267	701.2	629.1
35	0.2	400	1.327	574.1	558.3
17.5	0.2	450	1.439	547.6	541.3
52.5	0.15	400	1.158	580.1	517.8
35	0.1	400	1.274	405.4	480.1
35	0.2	500	1.357	591.1	578.1
17.5	0.1	450	1.351	391.8	466.5
35	0.15	450	1.283	569.5	521.1
52.5	0.1	450	1.189	596.7	499.8

Adequacy Assessment of the Model

An analytical model has been developed to evaluate the data obtained for all three response variables of linear type, considering the effects of average input parameters (Linear Vs. Means), as presented in Table 6. The confidence level of the model is set to be 95%; therefore, the values of R^2_{Adj} and R^2_{Pre} should ideally have a difference of less than 0.2 and be close to the confidence level. This criterion holds for the analytical models of maximum force and plastic strain. However, in the case of the variable maximum stress response, the difference between the above indicators is higher than 0.2, and their values with the specified confidence level are more different than those for the maximum force and plastic strain. However, since the P-value is less than 0.05, the proposed analytical model with high reliability can be applied to evaluate the data obtained for stress.

Table 6. The analytical model adapted to each of the output parameters, max PEEQ, max stress, and max punch force

	Source	Sequential p-value	Adjusted R^2	Predicted R^2	
Max PEEQ	Linear	<0.0001	0.9279	0.8902	Suggested
	2FI	0.9834	0.8946	0.7461	
	Quadratic	0.8266	0.8376		
	Cubic				Aliased
Max Stress	Linear	0.0143	0.5649	0.2890	Suggested
	2FI	0.1870	0.6904	0.1750	
	Quadratic	0.4400	0.7196		
	Cubic				Aliased
Max Punch Force	Linear	<0.0001	0.8877	0.8147	Suggested
	2FI	0.3183	0.9024	0.7302	
	Quadratic	0.4079	0.9166		
	Cubic				Aliased

The Adequate Precision index examines another criterion for evaluating the accuracy of data analysis by the model. This index measures the signal-to-noise ratio, which must be higher than 4. The values obtained by this index for stress, PEEQ, and maximum force are 7.028, 19.634, and 16.738, respectively.

Qualitative Study of Experimental Results

The assessment of data accuracy from the experiments is presented in Figure 7. The results do not follow any particular procedure or function, indicating the normal distribution of the data. The data close to the red line have been entirely covered by the analytical model, and the data that are vertically farther than the diagonal line shows the probable error in the obtained result (the error may be higher or lower depending on the vertical distance from the index axis).

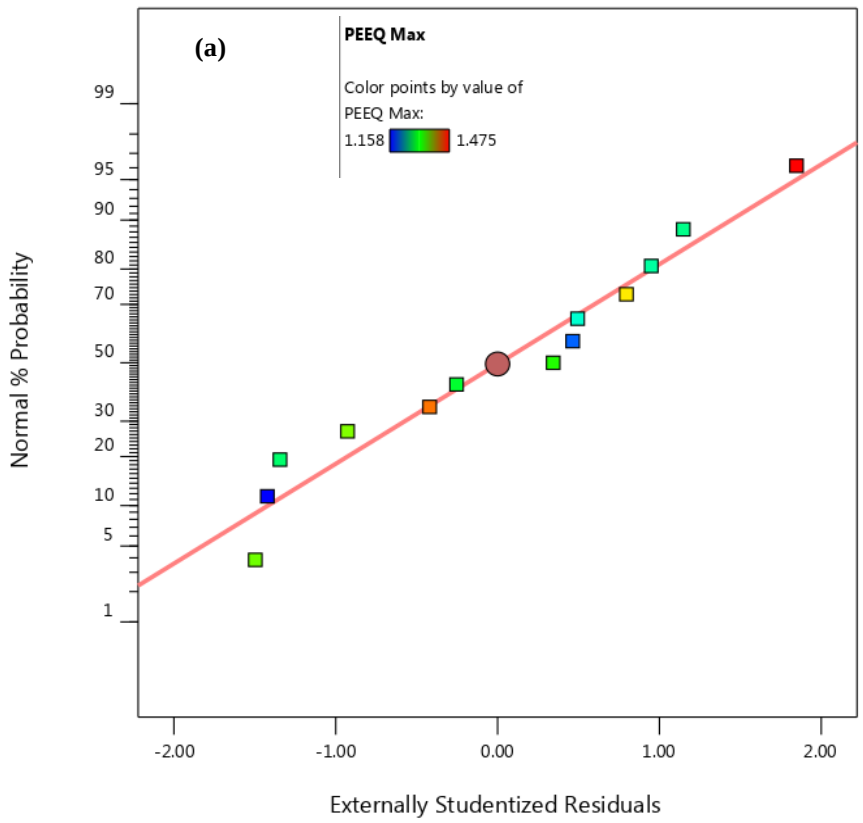

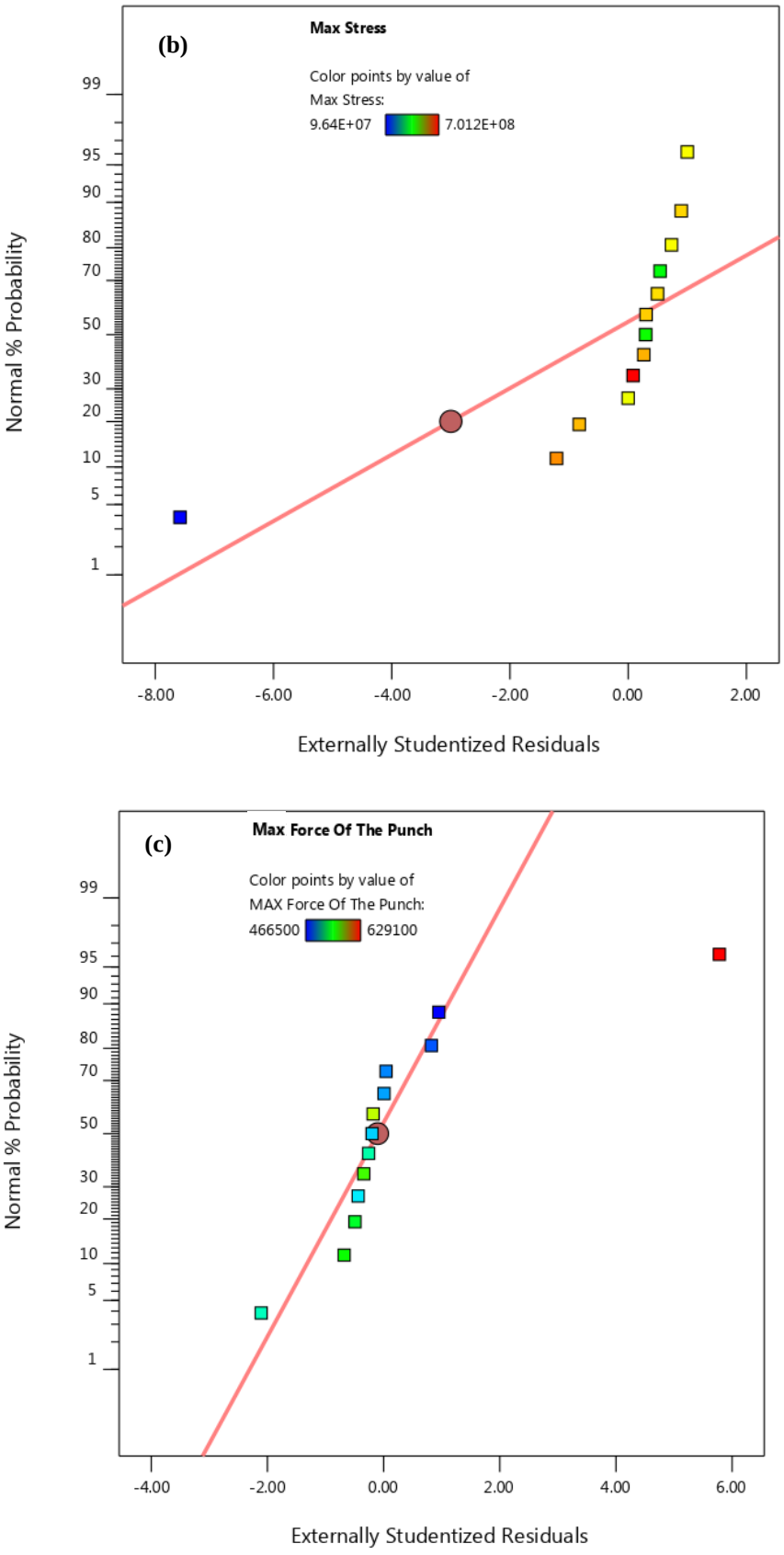

Figure 7. Normal probability plot for distribution of the studied result data

Moreover, by evaluating the data requirement index for transformation, it was concluded that since the coefficient of result variables falls in the acceptable range of 3 to 10, there is no need to transform this data, serving as additional evidence of the accuracy of the obtained result. It should be noted that this coefficient is computed from the ratio of the maximum to the minimum value of each response interval, which is equal to 1.27, 7.27, and 1.34 for PEEQ, the maximum stress, and the maximum required force by the process, respectively.

Parameters Effects on PEEQ

Table 7 indicates the analysis of variance and the effect coefficients related to the input parameters in the investigation of PEEQ. Figure 8 shows that punch speed reversely affected the considered output by 61.63%, and then the FC and BHF had the most extensive direct effects with 21.05% and 17.32%, respectively.

Table 7. Variance analysis and coefficients of the input parameters effect on PEEQ

Source	Sum of Squares	df	Mean Square	F-value	p-value	
Model	0.0959	3	0.0320	52.50	<0.0001	significant
Punch Speed	0.0802	1	0.0802	131.70	<0.0001	
FC	0.0094	1	0.0094	15.41	0.0035	
BHF	0.0063	1	0.0063	10.39	0.0104	
Residual	0.0055	9	0.0006			
Cor Total	0.1014	12				

Factor	Coefficient Estimate	df	Standard Error	95% CI Low	95% CI High	VIF
Intercept	1.31	1	0.0068	1.30	1.33	
Punch Speed	-0.1001	1	0.0087	-0.1199	-0.0804	1.0000
FC	0.0342	1	0.0087	0.0145	0.0540	1.0000
BHF	0.0281	1	0.0087	0.0084	0.0479	1.0000

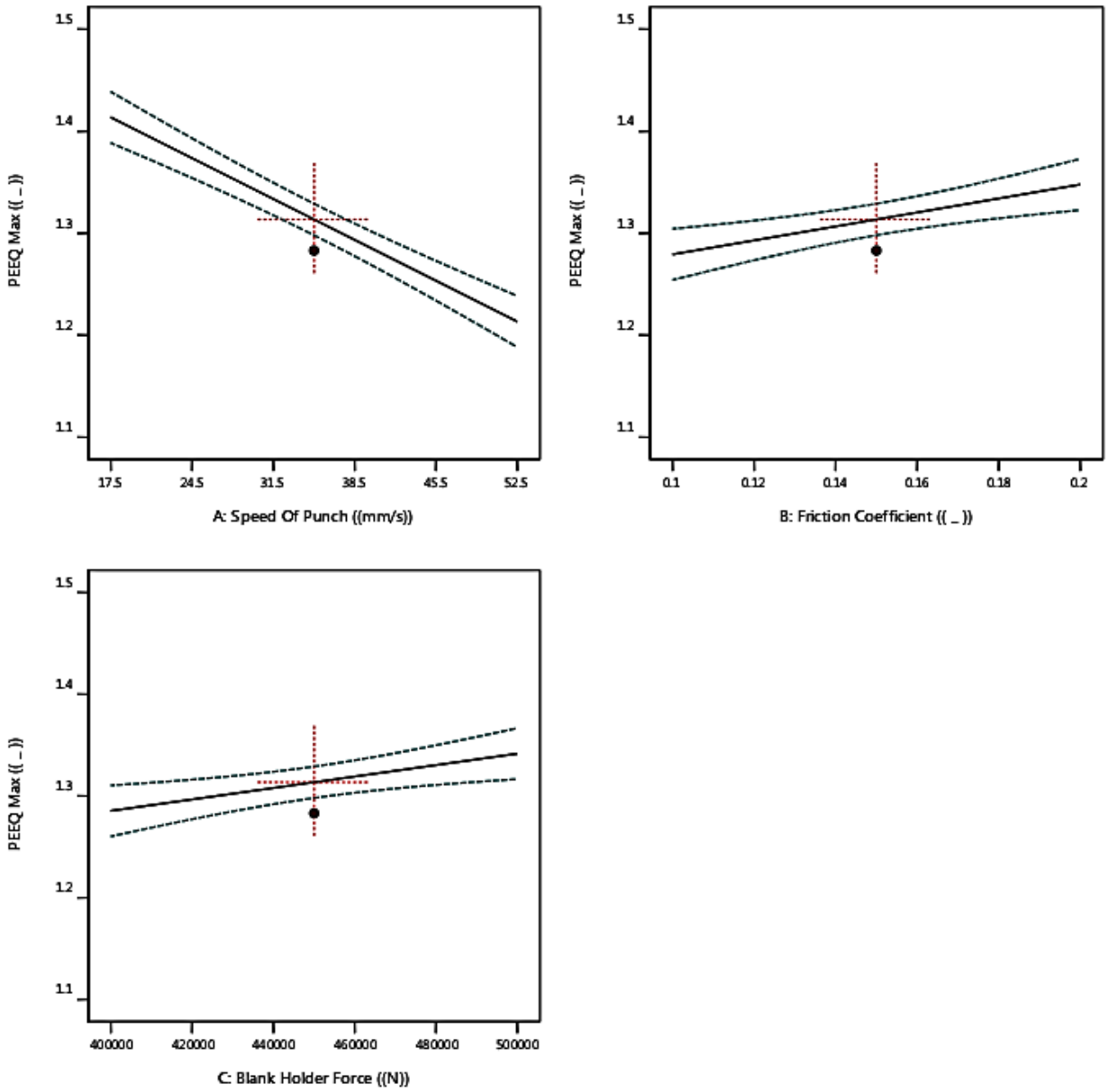

Figure 8. Relationship between control variables and PEEQ

Figure 9. shows the response surface recorded for PEEQ by considering the average BHF as a constant value. As shown in this Figure, the maximum value of plastic strain occurred in the end and back corners of the graph, i.e., at minimum punch speed and maximum FC.

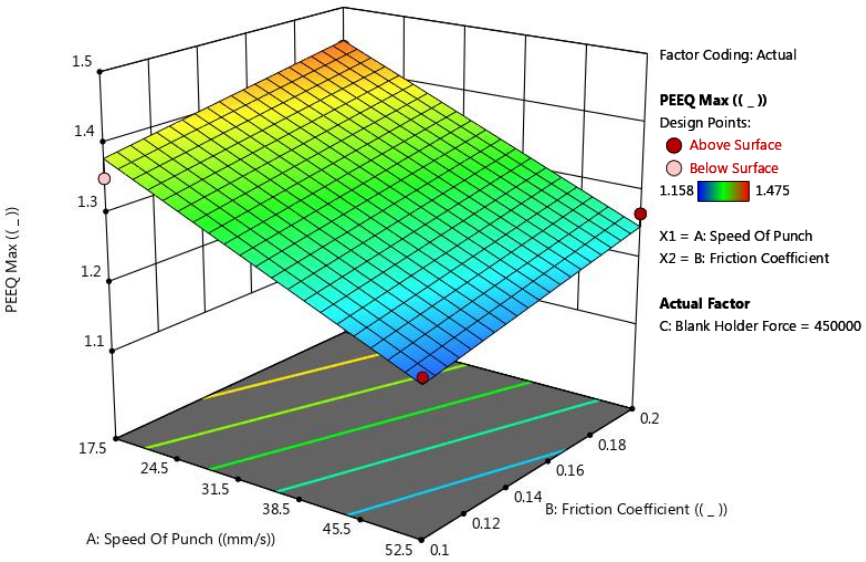

Figure 9. Three-dimensional surface plot of the relationship between the punch speed and FC parameters with PEEQ

Parameters Effects on Stress

Analysis of variance and regression equation coefficients of input variables affecting stress are presented in Table 8 and Figure 10. According to the relevant tables and figures, the punch velocity, BHF, and FC directly affected the stress output with contributions of 44.88%, 31.47%, and 23.65%, respectively.

Table 8. Analysis of variance and coefficients of the effect of input parameters on maximum stress

Source	Sum of Squares	df	Mean Square	F-value	p-value	
Model	1.840E+17	3	6.134E+16	6.19	0.0143	significant
Punch Speed	1.041E+17	1	1.041E+17	10.51	0.0101	
FC	2.884E+16	1	2.884E+16	2.91	0.1221	
BHF	5.112E+16	1	5.112E+16	5.16	0.0492	
Residual	8.913E+16	9	9.903E+15			
Cor Total	2.731E+17	12				

Factor	Coefficient Estimate	df	Standard Error	95% CI Low	95% CI High	VIF
Intercept	5.199E+08	1	2.760E+07	4.574E+08	5.823E+08	
Punch Speed	1.140E+08	1	3.518E+07	3.446E+07	1.936E+08	1.0000
FC	6.004E+07	1	3.518E+07	-1.955E+07	1.396E+08	1.0000
BHF	7.994E+07	1	3.518E+07	3.453E+05	1.595E+08	1.0000

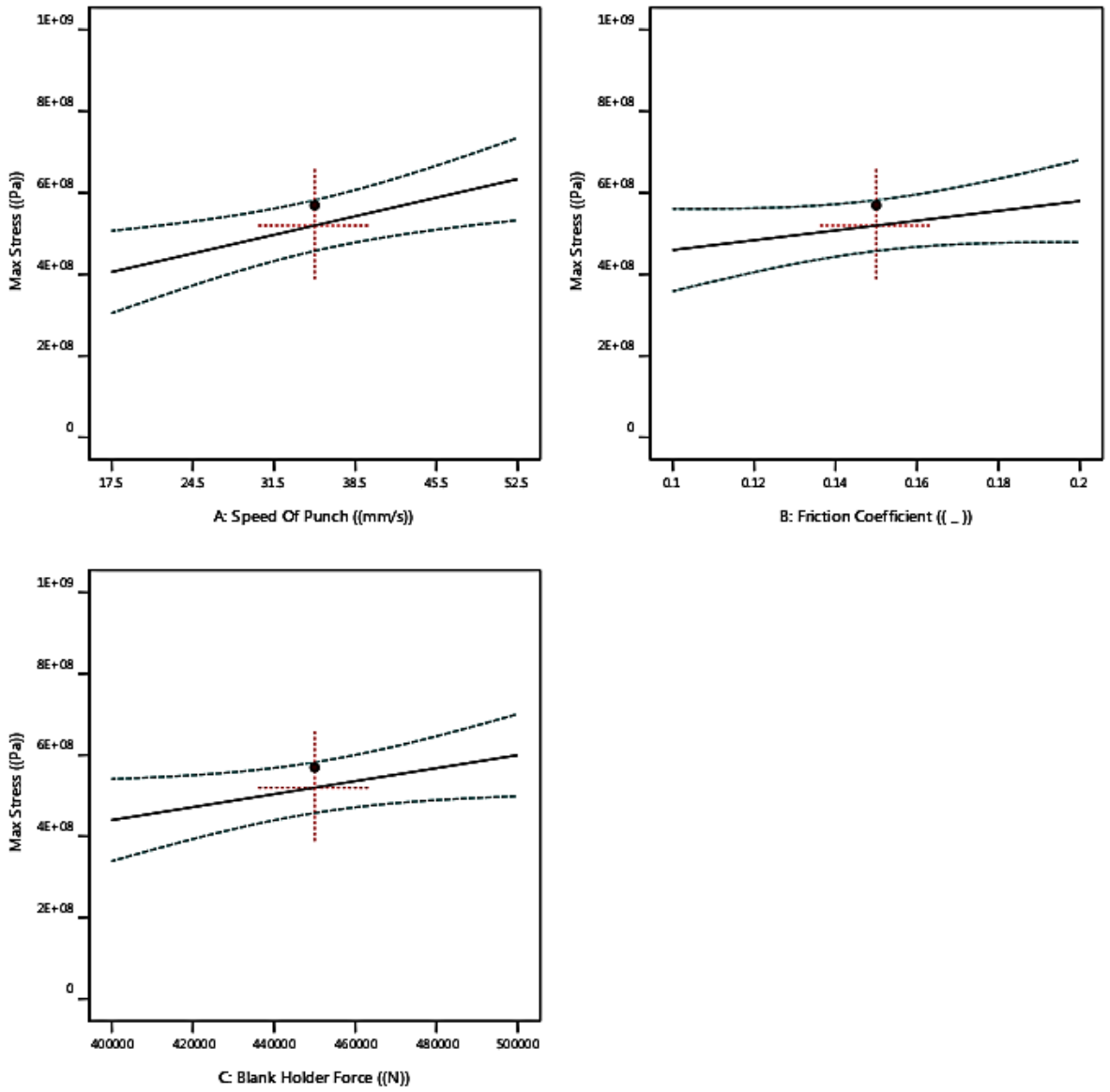

Figure 10. Relationship between stress and process control inputs

The Box–Behnken provides modeling of the response surface. These designs are not based on complete or fractional factorial designs. The design points are positioned in the middle of the subareas. The points are located in the middle of the edges of the experimental domain. Figure 11 demonstrates the maximum stress values for each of the 12 midpoints and center points evaluated in the experiment.

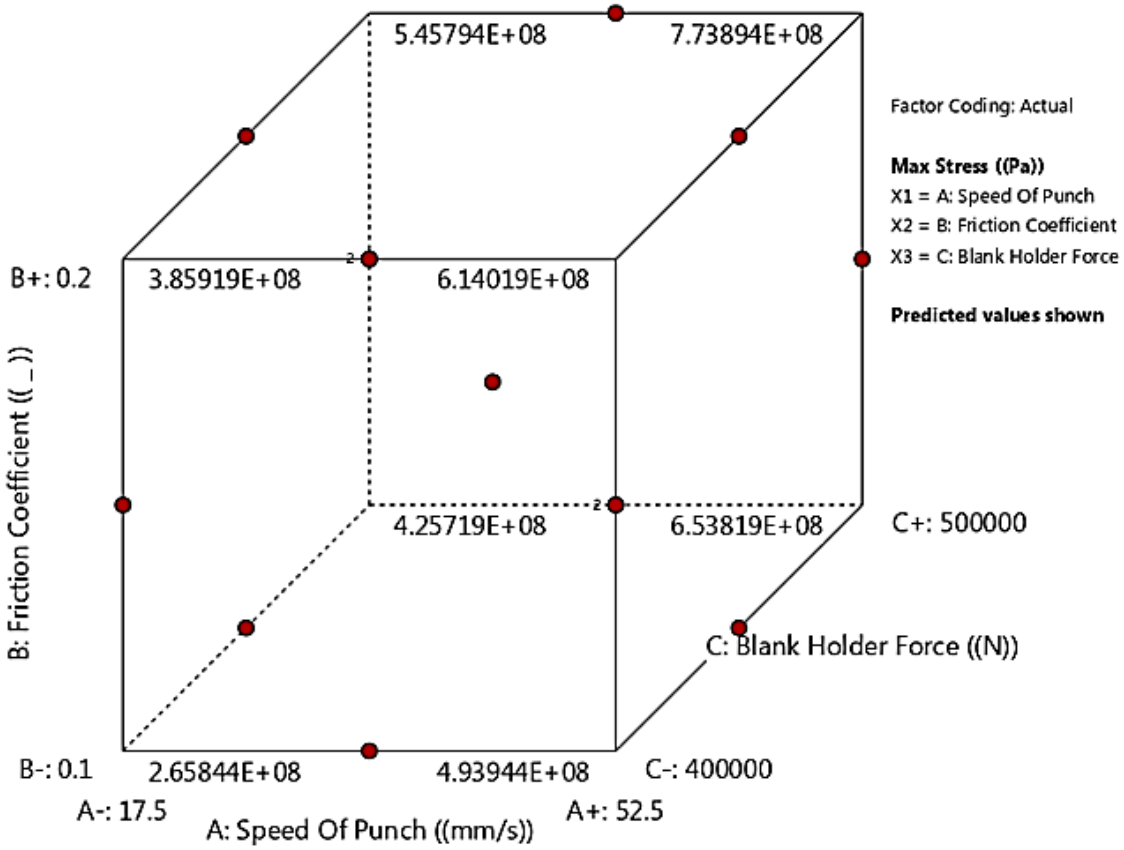

Figure 11. Cube graph of the results obtained for the maximum value of stress

Parameters Effects on Force

According to the results obtained from Table 9, each of the input parameters, punch speed, FC, and BHF, directly contributed to the force variations by 30.14%, 58.69%, and 11.15%, respectively. This behavior means that the maximum force required for the process increases with the increase of each of these input components (Figure 12).

Table 9. Analysis of variance and coefficients of the effect of control variables on the maximum force required for the process

Source	Sum of Squares	df	Mean Square	F-value	p-value	
Model	2.255E+10	3	7.515E+09	32.61	<0.0001	significant
Punch Speed	4.574E+09	1	4.574E+09	19.85	0.0016	
FC	1.734E+10	1	1.734E+10	75.26	<0.0001	
BHF	6.266E+08	1	6.266E+08	2.72	0.1336	
Residual	2.074E+09	9	2.305E+08			
Cor Total	2.462E+10	12				
Factor	Coefficient Estimate	df	Standard Error	95% CI Low	95% CI High	VIF
Intercept	5.251E+05	1	4210.449	5.155E+05	5.346E+05	
Punch Speed	23912.50	1	5367.34	11770.74	36054.26	1.0000
FC	46562.50	1	5367.34	34420.74	58704.26	1.0000
BHF	8850.00	1	5367.34	-3291.76	20991.76	1.0000

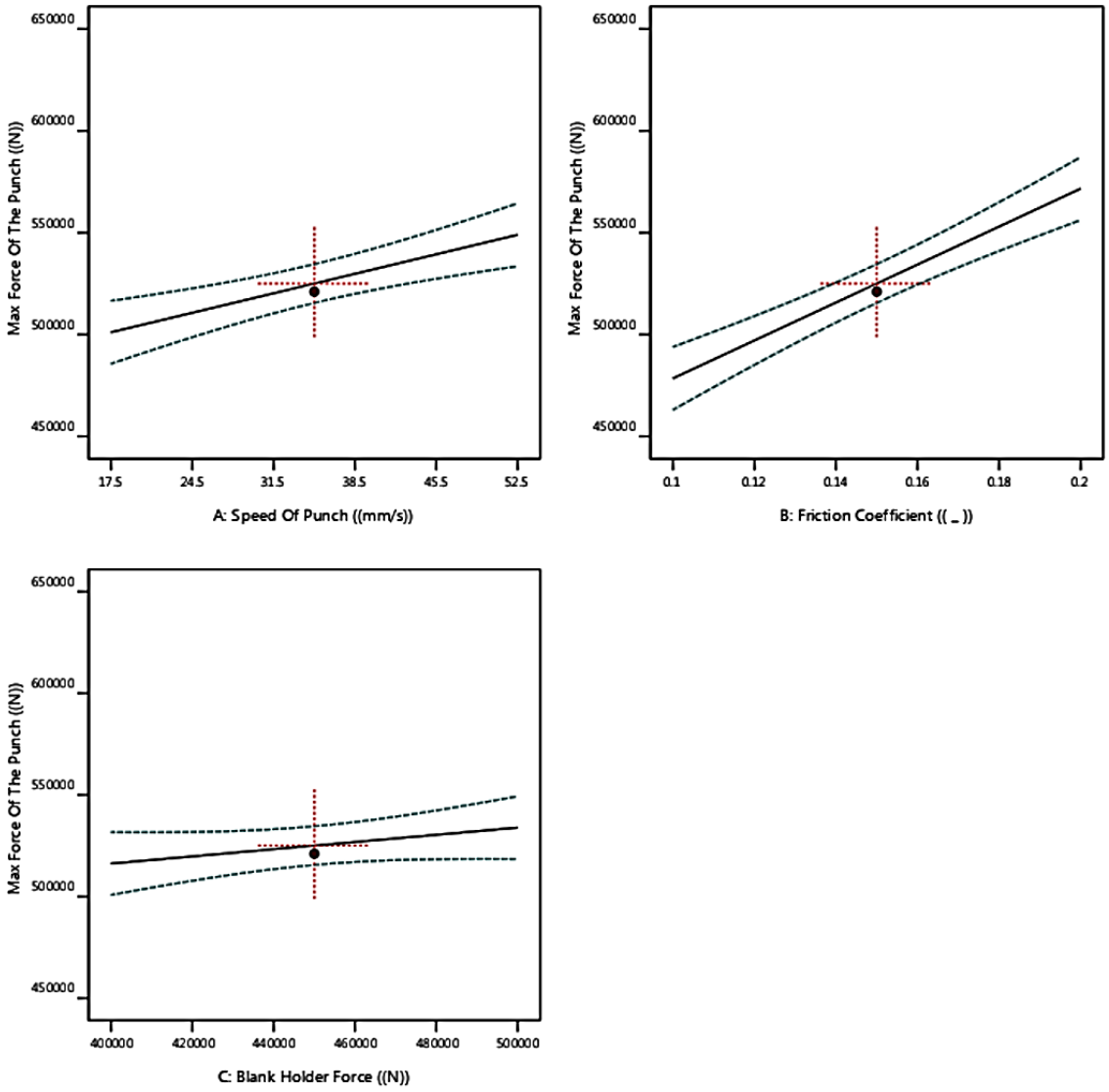

Figure 12. Relationship between process control parameters and force

Figure 13 indicates the changes in force relative to the variations in the two inputs affecting the force, the FC, and the punch speed in the form of color contour. In this contour, where the BHF is considered fixed and equal to 450,000 (N), the punch has the highest value of force with increasing the FC and punch speed in the proper and upper corner areas, and the punch force also has decreased by reducing these two parameters in the lower and left corners. Obviously, in the investigated range of variables, the changing rate of the force is more significant when FC varies. Then, it can be concluded that in the constant value of BHF (450,000N), the effect of FC on the punch force is more than punch speed.

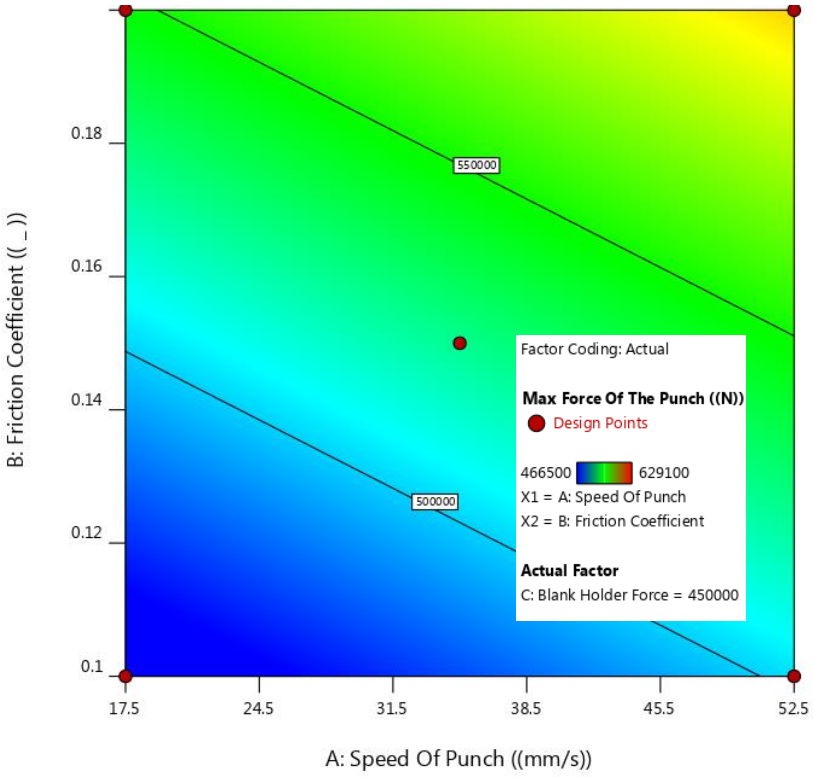

Figure 13. The contour of the relationship between punch speed and FC with force required for the process

4. Conclusion

In the present investigation, the forming process of the first stage of the Kia Rio's jack bracket was analyzed using FE simulation, practical tests, and the DOE method. Thirteen different experiments were designed and carried out using the Box-Behnken response surface methodology to identify the type and extent of the effect of each process control parameter. The summary of the results is as follows:

1) The sheet's strength against tensile forces during the process causes the concentration of annular stresses in the edge area of the sheet and, ultimately, the shrinking phenomenon. The best solution to reduce the shrinkage is to increase the BHFs. These tensile forces also lead to the rupture at the contact surface of the sheet with the punch. The deformation rate should be selected according to the material's yield strength to prevent the sheet from rupture.

2) The maximum value of plastic strain occurs in the locations of the protrusions and depressions on the part surface. In other areas, the deformations are often elastic.

3) A direct relationship exists between the maximum required force and each input parameter. FC, punch speed, and BHF affect the force by 58.69%, 30.14%, and 11.15%, respectively. The instantaneous gradient of the force vs. time curve experiences a considerable change. It has the highest value in the final seconds of the process due to the yield strength of the material.

4) There is a direct relationship between the maximum stress of the final part and each of the parameters. Punch speed, BHF, and FC affected the maximum stress developed throughout the process by 44.88%, 31.47%, and 23.65%, respectively.

5) There is an inverse relationship between punch speed and the plastic strain of the part, and its reduction had a 61.63% effect on increasing the plastic strain. The two parameters, FC and BHF, have affected the variations of the mentioned response by 21.05% and 17.32%, respectively.

5. References

[1] Hashemian, S., Keshtiban, P. M. and Oskui, A. 2022. Fracture Behavior of the Forged Aluminum 7075-T6 Alloy under Mixed-Mode Loading Conditions. Engineering Failure Analysis. 140: 106610. doi: 10.1016/j.engfailanal.2022.106610.

[2] Hashemian, S., Keshtiban, P.M. and Oskui, A. 2022. Numerical Simulation of Hot Forging Process of KIA Car Brake's Output Shaft. ADMT Journal. 15(1): 115-124. doi: 10.30486/admt.2022.1933346.1290.

[3] Alimirzaloo, V., Biglari, F. R., Sadeghi, M. H. et al. 2019. A Novel Method for Preform Die Design in Forging Process of an Airfoil Blade based on Lagrange Interpolation and Meta-heuristic Algorithm. International Journal of Advanced Manufacturing Technology. 102(9): 4031-4045. doi: 10.1007/s00170-019-03512-9.

[4] Taghavi, V., Alimirzaloo, V., Soleimanpur, M., et al. 2020. An Investigation of the Effective Factors in the Shape Rolling Process of a Compressor Blade. Iranian Journal of Materials Forming. 7(2):16-25. doi: 10.22099/ijmf.2020.37104.1156.

[5] Keshtiban, P. M., Taher, A. and Keshtiban, M. M. 2021. Practical Study and Finite Element Simulation of Production Process of the Bush of Gearbox of Mercedes-Benz 10-wheel Truck by Closed Die Forging. Journal of Computational Applied Mechanics. 52(1): 69-84. doi: 10.22059/jcamech.2020.312296.568.

[6] Keshtiban, P. M., Behnagh, R. and Alimirzaloo, V. 2018. Routes Investigation in Equal Channel Multi-angular Pressing Process of UFG Al− 3% Mg Alloy Strips. Transactions of the Indian Institute of Metals. 71(3): 659-664. doi: 10.1007/s12666-017-1198-3.

[7] Hein, P. 2005. A Global Approach of the Finite Element Simulation of Hot Stamping. Advanced Materials Research. 6: 763-770. doi: 10.4028/www.scientific.net/AMR.6-8.763.

[8] Firat, M. 2007. Computer Aided Analysis and Design of Sheet Metal Forming Processes: Part I– The Finite Element Modeling Concepts. Materials & Design. 28(4): 1298-1303. doi: 10.1016/j.matdes.2006.01.026.

[9] Zhang, P., Zhu, L., Luo, S. et al. 2019. Hot Stamping Forming and Finite Element Simulation of USIBOR1500 High-Strength Steel. The International Journal of Advanced Manufacturing Technology. 103(5): 3187-3197. doi: 10.1007/s00170-019-03727-w.

[10] Keshtiban, P. M. and Bashirzadeh, F. 2022. Constitutive Analysis and Hot Deformation Behavior of Homogenized Al-3Mg Alloy. JOM. 75: 905-913. doi: 10.1007/s11837-022-05648-8.

[11] Kim, K. J. 2021. Lightweight Design and Fatigue Characteristics of Automotive Knuckle by Using Finite Element Analysis. Journal of Mechanical Science and Technology. 35(7): 2989-2995. doi: 10.1007/s12206-021-0622-0.

[12] Zhou, J., Yang, X-ming et al. 2021. Numerical Simulation and Experimental Investigation of Tailored Hot Stamping of Boron Steel by Partial Heating. Journal of Materials Research and Technology. 14: 1347-1365. doi: 10.1016/J.JMRT.2021.07.025.

[13] Wang, H., Chen, G., Zhu, Q. et al. 2024. Frictional Behavior of Pure Titanium Thin Sheet in Stamping Process: Experiments and Modeling. Tribology International. 191: 109131. doi: 10.1016/j.triboint.2023.109131.

[14] Modanloo, V., Mashayekhi, A. and Akhoundi, B. 2024. A Comparative Analysis of Predictive Models for Estimating the Formability of Stamped Titanium Bipolar Plates for Proton Exchange Membrane Fuel Cells. International Journal of Hydrogen Energy. 56: 894-902. doi: 10.1016/j.ijhydene.2023.12.242.

[15] Dhinesh, K., SubhaSankari, T., Paneerselvam, T. et al. 2019. Simulation and Numerical Analysis of Warm Stamping (AA6061). Materials Today: Proceedings. 16: 598-603. doi: 10.1016/j.matpr.2019.05.134.

[16] Silva, M. B., Baptista, R. and Martins, P. 2004. Stamping of Automotive Components: a Numerical and Experimental Investigation. Journal of Materials Processing Technology. 155: 1489-1496. doi: 10.1016/J.JMATPROTEC.2004.04.208.

[17] Bidgoli, M. O., Kashyzadeh, K. R., Rahimian Koloor, S. S. et al. 2020. Optimum Design of Sunken Reinforced Enclosures under Buckling Condition. Applied Sciences, 2020. 10(23): 8449. doi: 10.3390/app10238449.

[18] Eghbalian, M., Ansari, R., Bidgoli, M. O. et al. 2022. Finite Element Investigation of the Geometrical Parameters of Waviness Carbon Nanotube on Directional Young's and Shear Elastic Modulus of Polymer Nanocomposites. Journal of The Institution of Engineers (India): Series D: 1-14. doi: 10.1007/s40033-022-00414-1.

[19] Naeini, M. M., Moghadasi, S. M. and Bidgoli, M. O. 2018. A Numerical Analysis of Reinforced T Shaped Concrete Beams by Polymeric Strap of CFRP and GFRP with Finite Element Method Technique. Civil Engineering Journal. 4(5): 1006-1018. doi: 10.28991/CEJ-0309152.

[20] Zhang, Q. , Zhang, S. and Li. J. 2017. Three Dimensional Finite Element Simulation of Cutting Forces and Cutting Temperature in Hard Milling of AISI H13 Steel. Procedia Manufacturing. 10: 37-47. doi: 10.1016/j.promfg.2017.07.018

[21] Öztürk, G. 2010. Numerical and Experimental Investigation of Perforation of ST-37 Steel Plates by Oblique Impact. 2010, Middle East Technical University. Msc thesis.

[22] Hasanzadeh, H., Mohtarami, E., Bidgoli, M. O. et al. 2022. Collapse Analysis of Al 6061 Alloy Conical Shells with Circular Cutouts under Axial Loading: Experiment and Simulation. Proceedings of the Institution of Mechanical Engineers, Part L: Journal of Materials: Design and Applications. 236(4): 704-714. doi: 10.1177/14644207211054655

[23] Shang, J. and Daehn, J. 2011. Electromagnetically Assisted Sheet Metal Stamping. Journal of Materials Processing Technology. 211(5): 868-874. doi: 10.1016/j.jmatprotec.2010.03.005.